SCIENTIFIC REPORTS

OPEN

Superconductivity in Ti_4O_7 and γ-Ti_3O_5 films

K. Yoshimatsu[1], O. Sakata[2,3] & A. Ohtomo[1,3]

Received: 5 July 2017
Accepted: 14 September 2017
Published online: 02 October 2017

Titanium dioxide is one of the most popular compounds among simple oxides. Except for the fully oxidized titanate, titanium oxides have partially filled *d* states and their exotic properties have captured attention. Here, we report on the discovery of superconductivity in Ti_4O_7 and γ-Ti_3O_5 in a thin film form. The epitaxial Ti_4O_7 and γ-Ti_3O_5 thin films were grown using pulsed-laser deposition on $(LaAlO_3)_{0.3}$–$(SrAl_{0.5}Ta_{0.5}O_3)_{0.7}$ and α-Al_2O_3 substrates, respectively. The highest superconducting transition temperatures are 3.0 K and 7.1 K for Ti_4O_7 and γ-Ti_3O_5, respectively. The mechanism behind the superconductivity is discussed on the basis of electrical measurements and previous theoretical predictions. We conclude that the superconductivity arises from unstabilized bipolaronic insulating states with the assistance of oxygen non-stoichiometry and epitaxial stabilization.

In the periodic table, titanates are the first group of simple oxides, which are defined as oxides consisted of a kind of the cation and oxygen ion(s), indicating metallicity, and all the simple oxides of scandium or much lighter elements are insulating. Therefore, the choice of titanates is favourable for large electron–phonon coupling. Figure 1(a) shows a schematic of the crystal structure for Ti_4O_7. Ti_4O_7 is the first member of Magnéli phase [a triclinic cell ($a = 5.597$ Å, $b = 7.125$ Å, $c = 20.429$ Å, $\alpha = 67.7°$, $\beta = 57.16°$, $\gamma = 108.76°$)][1,2] that exhibits unique low-dimensional structures characterized by shear planes. These shear planes correspond to the rutile TiO_2 (121) planes and amputate the edge-shared infinite TiO_6 chains at every n TiO_6 blocks with shifting by a half of the unit cell. In the nominal composition, a TiO_6 tetramer has two electrons occupying the Ti 3*d* states. Trititanium pentoxide (Ti_3O_5) with polymorphisms (α-, β−, γ−, δ−, and λ-phases) is a neighbour of the Magnéli phase[3–7]. γ-Ti_3O_5 is one of them with a monoclinic cell ($a = 5.0747$ Å, $b = 9.9701$ Å, $c = 7.1810$ Å, $\alpha = 109.865°$)[4]. In contrast to the Magnéli phase, there are no shear planes, as illustrated in Fig. 1(b). However, since the chemical formula is consistent with that of the Magnéli phase (Ti_nO_{2n-1} at $n = 3$), it is sometimes designated as the first member of the Magnéli phase. Because of difficulty in the growth of a single crystal due to polymorphism, their physical properties are still under debate. Several studies have dealt with the structural phase transitions accompanying MIT, which are induced under the specific conditions ($\alpha \leftrightarrow \beta$ at 450 K[3], $\delta \leftrightarrow \gamma$ at 240 K[4–7], and $\beta \leftrightarrow \lambda$ by irradiation using visible-light pulses[6]).

We find that Ti_4O_7 and γ-Ti_3O_5 films synthesized using epitaxial growth are superconductors with T_Cs 3.0 K and 7.1 K, respectively. The temperature dependence of resistivity strongly depended on the growth atmosphere. The Ti_4O_7 film grown under a more oxidation condition of oxygen atmosphere exhibited metal–insulator transition (MIT) accompanied by clear hysteresis at ~150 K. The insulating phase was suppressed in the films grown under a less oxidative condition of Ar atmosphere, and the superconducting phase appeared at low temperatures. These results and the previous theoretical prediction suggest that epitaxial stabilization and oxygen non-stoichiometry play key roles in the realization of superconductivity in these titanates.

Results

Structural characterization. The formation of the Ti_4O_7 and γ-Ti_3O_5 phases was verified using x-ray diffraction (XRD). The out-of-plane XRD patterns showed intense reflections from the Ti_4O_7 films grown on $(LaAlO_3)_{0.3}$–$(SrAl_{0.5}Ta_{0.5}O_3)_{0.7}$(LSAT) (100) substrates and the γ-Ti_3O_5 film grown on α-Al_2O_3 (0001) substrates [Fig. 2(a) and (b), respectively]. These substrates are insulating, non-magnetic, and exhibit high reduction resistance, providing advantages in the growth and search of a superconducting sample. Irrespective of the growth condition, Ti_4O_7 202 reflection was detected at $2\theta = 42.38°$, corresponding to $d_{202} = 2.13$ Å. No other film reflections except for the 404 reflection at $2\theta = 92.60°$ was detected in wide-range XRD patterns. The γ-Ti_3O_5 022 reflection

[1]Department of Chemical Science and Engineering, Tokyo Institute of Technology, 2-12-1 Ookayama, Meguro-ku, Tokyo, 152-8552, Japan. [2]Synchrotron X-ray Station at SPring-8, National Institute for Materials Science (NIMS), 1-1-1 Koto, Sayo-cho, Sayo-gun, Hyogo, 679-5148, Japan. [3]Materials Research Center for Element Strategy (MCES), Tokyo Institute of Technology, 4259 Nagatsuta-cho, Midori-ku, Yokohama, 226-8503, Japan. Correspondence and requests for materials should be addressed to K.Y. (email: k-yoshi@apc.titech.ac.jp)

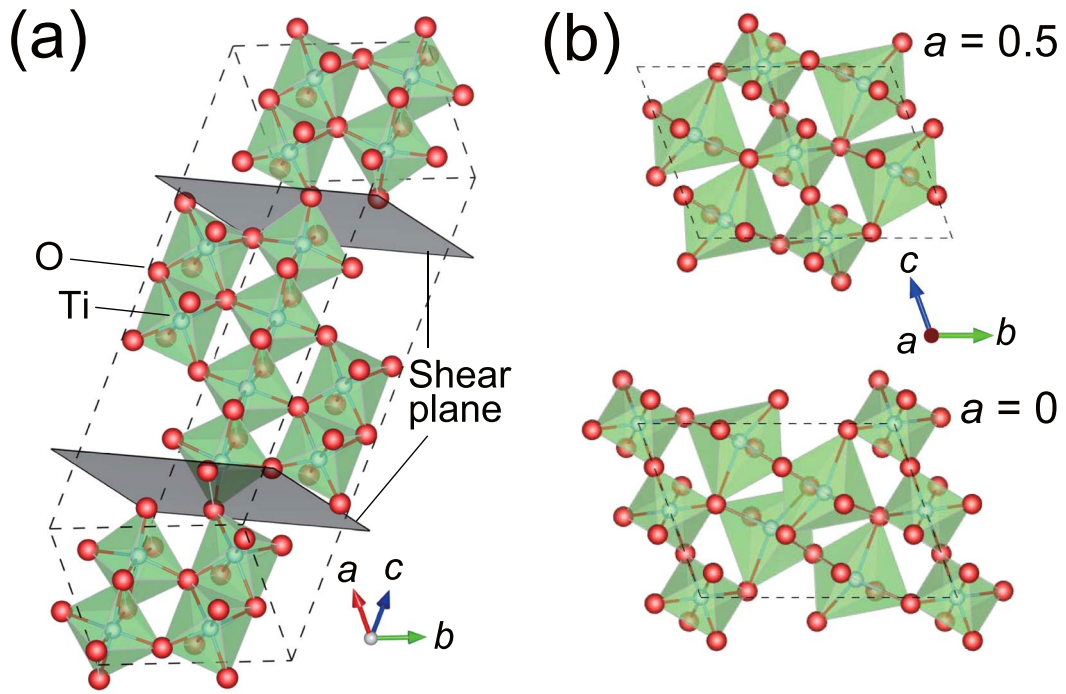

Figure 1. Crystal structures of titanates. Schematics of the crystal structures for (**a**) the first member of Magnéli-phase Ti_4O_7 and (**b**) γ-Ti_3O_5.

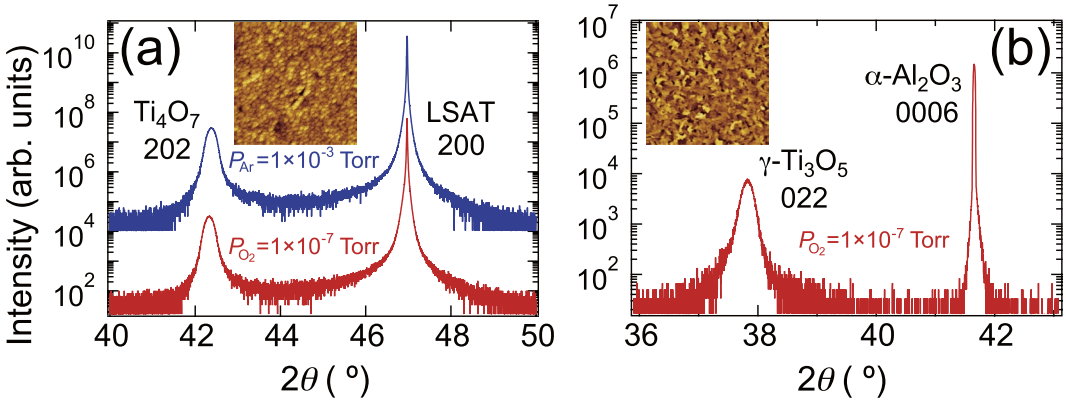

Figure 2. Structural characterization of titanate films. (**a**) Out-of-plane XRD patterns for Ti_4O_7 films grown on LSAT (100) substrates under Ar gas at 1×10^{-3} Torr (top) and under oxygen gas at 1×10^{-7} Torr (bottom). (**b**) Out-of-plane XRD pattern for the γ-Ti_3O_5 film grown on α-Al_2O_3 (0001) substrates under oxygen gas at 1×10^{-7} Torr. The insets show AFM images (5 μm × 5 μm) taken for the same films. Colour codes are 13 nm and 8 nm in height for (**a**) and (**b**), respectively.

was detected at $2\theta = 37.83°$, corresponding to $d_{022} = 2.38$ Å. The out-of-plane single orientation was verified using wide-range XRD patterns (not shown). Surface morphology of the films are shown in the inset of Fig. 2. The small grains were observed and the root mean square roughness was about 1 nm for both films. Their surface morphology was different from that of TiO and Ti_2O_3 (see Fig. S1 in Supplementary information)[8].

Because of various polymorphisms with different ratios of oxygen to titanium, their crystal structures must be carefully distinguished. Then, we used the tilt angle χ-dependence of 2θ-θ XRD profiles to survey the asymmetric film reflections (see Figs S2 and S6 in Supplementary Information). Reflections coming from the substrate and film were found at characteristic χ angles. Since the intensities of the film reflections were too weak to determine the d values of interplanar spacing precisely, synchrotron radiation XRD measurements were also performed (see Figs S3–S5,S7 and S8 in Supplementary Information). From the d values and χ angles, we identified the Miller indices as those listed in Tables S2 and S3. In comparison to the previous structural analyses of titanates[1–7], we concluded that the films grown on LSAT (100) and α-Al_2O_3 (0001) substrates were Ti_4O_7 and γ-Ti_3O_5, respectively. Furthermore, using the d values and Miller indices (Tables S1 and S3), we evaluated lattice parameters of our titanate films: Ti_4O_7 film grown under $P_{O2} = 1 \times 10^{-7}$ Torr ($a = 5.52$ Å, $b = 7.12$ Å, $c = 20.43$ Å, $\alpha = 67.5°$,

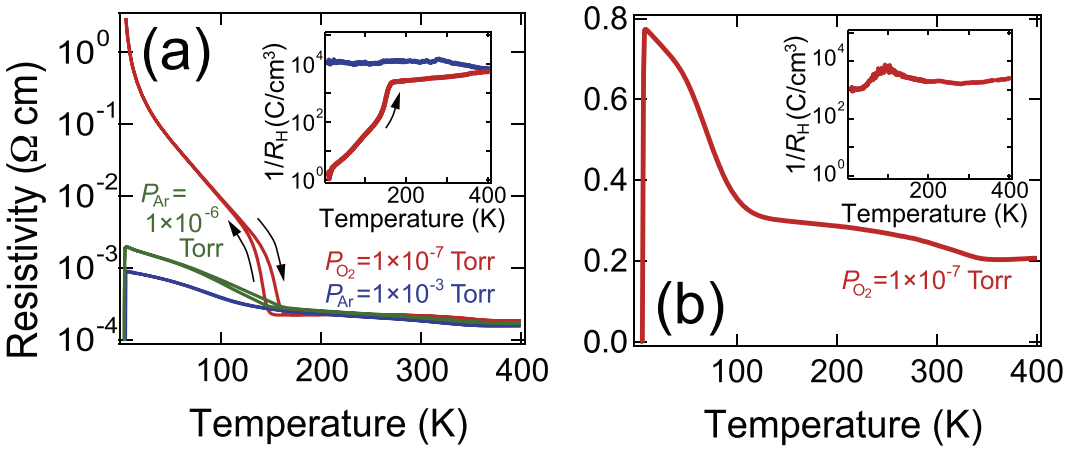

Figure 3. Temperature dependence of resistivity of titanate films. (**a**) Temperature dependence of resistivity for Ti_4O_7 films grown under three different conditions. The inset shows the temperature dependence of the Hall measurement. (**b**) Temperature dependence of resistivity for the γ-Ti_3O_5 film. The inset shows the temperature dependence of the Hall measurement.

$\beta = 57.3°$, $\gamma = 108.8°$), Ti_4O_7 film grown under $P_{Ar} = 1 \times 10^{-7}$ Torr ($a = 5.52$ Å, $b = 7.11$ Å, $c = 20.46$ Å, $\alpha = 67.5°$, $\beta = 57.2°$, $\gamma = 108.8°$), and γ-Ti_3O_5 film ($a = 4.99$ Å, $b = 9.80$ Å, $c = 7.06$ Å, $\alpha = 110.3°$). The a-axis lattice constant of both Ti_4O_7 films is smaller than that of bulk. In contrast, b- and c-axes lattice constants of the former Ti_4O_7 films were in agreement with those of bulk. The b- (c-) axis lattice constant of the latter Ti_4O_7 film was smaller (larger) than that of bulk. We note that the c-axis length directly corresponds to the Ti–Ti bond length in the TiO_6 tetramer [see Fig. 1(a)] and c-axis lattice constant of the former Ti_4O_7 film is larger than that of the latter Ti_4O_7 film. For the γ-Ti_3O_5 film, all of the lattice constants were smaller than those of bulk. The lattice parameters of the titanate films and bulk are listed in Tables S2 and S4 for comparison.

Formation of the different titanate phases under the identical growth condition suggests that epitaxial effects play an important role for stabilizing the Ti_4O_7 and γ-Ti_3O_5 films on each substrate (see Fig. S9 in Supplementary Information). In fact, we have grown neither γ-Ti_3O_5 films on LSAT (100) substrates nor Ti_4O_7 films on α-Al_2O_3 (0001) substrates. The in-plane epitaxial relationship between the substrates and films were also investigated and described in Supplementary Information.

Temperature dependence of resistivity. The electrical properties of the films were investigated using the temperature dependence of resistivity (Fig. 3). The resistivity curves strongly depended on the growth atmosphere for Ti_4O_7 films [Fig. 3(a)]. For the film grown under $P_{O2} = 1 \times 10^{-7}$ Torr, MIT accompanied by clear hysteresis was found at around 150 K, which is in agreement with the behaviour of a bipolaron insulator of bulk Ti_4O_7[9–11]. In contrast, the insulating behaviours were strongly suppressed for the film grown under $P_{Ar} = 1 \times 10^{-3}$ Torr; the upturn in resistivity was weak. The different behaviour across MIT was in agreement with the difference in c-axis lattice constants of the Ti_4O_7 films: the larger c-axis length weakened the Ti^{3+}–Ti^{3+} bond in the TiO_6 tetramers for the Ti_4O_7 films grown under $P_{Ar} = 1 \times 10^{-3}$ Torr. The weak resistivity upturn was also reported on V-doped bulk Ti_4O_7[12]. When V content exceeds 0.35 at%, the disordered bipolarons dominate the electronic properties in the insulating phase. If we account for the lower degree of oxidation at $P_{Ar} = 1 \times 10^{-3}$ Torr, oxygen deficiency would play a similar role to substitution of the Ti site with V and be responsible for the suppression of the insulating states. Furthermore, superconductivity was observed at low temperatures. The Ti_4O_7 film grown under an intermediate condition ($P_{Ar} = 1 \times 10^{-6}$ Torr) exhibited both hysteresis and superconducting characteristics in the resistivity curve (also see Fig. S10 in Supplementary Information). We will refer to the Ti_4O_7 films grown under $P_{O2} = 1 \times 10^{-7}$ Torr ($P_{Ar} = 1 \times 10^{-3}$ Torr) as insulating (superconducting) ones in the following discussion.

The variation in the Hall coefficient (R_H) during warming exhibited a tendency similar to that of resistivity. At 300 K (10 K), the inverse R_H was 3.6×10^3 (1.5) and 1.2×10^4 (1.2×10^4) C/cm^3 for the films grown under $P_{O2} = 1 \times 10^{-7}$ Torr and $P_{Ar} = 1 \times 10^{-3}$ Torr, respectively. For the insulating Ti_4O_7 film, the temperature dependence of the inverse R_H [inset of Fig. 3(a)] suddenly decreased at around 150 K, suggesting that the MIT was induced by the depletion of hole carriers. The inverse R_H at 10 K was four orders of magnitude smaller than that at 300 K. The MIT in the bulk is associated with the formation of bipolarons[9–11], which remains robust in the insulating Ti_4O_7 film at low temperatures. In contrast, the inverse R_H for the superconducting Ti_4O_7 film was almost independent of temperatures, and even the value at 10 K was comparable to that at 300 K, suggesting the suppression of a bipolaronic insulating state.

The temperature dependence of the resistivity for the γ-Ti_3O_5 film exhibited a complex curve along three electronic phase transitions: MIT around 350 K, insulator–insulator transition around 100 K, and superconducting transition [Fig. 3(b)]. The intermediate transition would be related to the MIT of Ti_4O_7 due to their similar transition temperatures. Nevertheless, the resistivity upturn was much weaker, suggesting the suppression of the insulating states, as with the case of the superconducting Ti_4O_7 film. The inverse R_H almost [inset of Fig. 3(b)] remained the same (~10^3 cm^3/C) over the entire temperature range. The sign and magnitude of the R_H also reflected this correspondence.

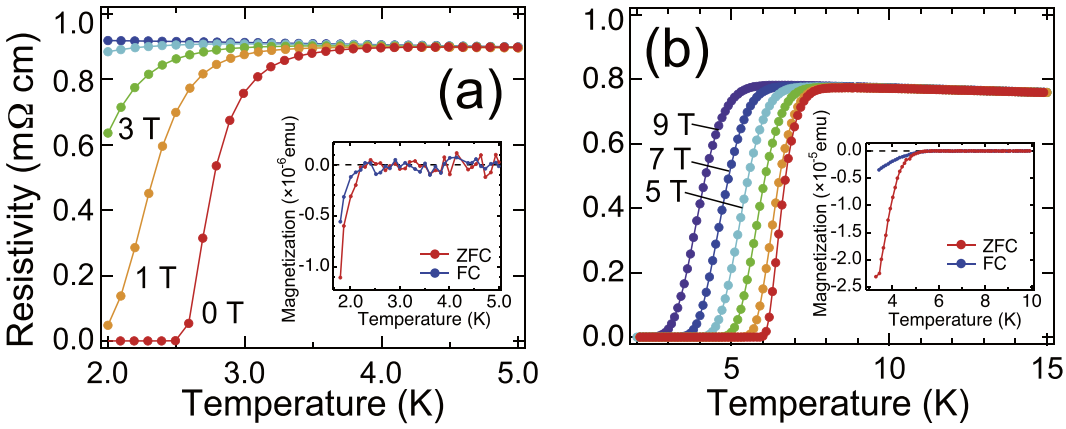

Figure 4. Superconducting properties of titanate films. (**a**) Temperature dependence of resistivity of the Ti_4O_7 film grown under $P_{Ar} = 1 \times 10^{-3}$ Torr at low temperatures. (**b**) Temperature dependence of resistivity of the γ-Ti_3O_5 film at low temperatures. The insets of (**a**) and (**b**) show temperature dependence of magnetization for (**a**) the superconducting Ti_4O_7 and (**b**) γ-Ti_3O_5 films at low temperatures, respectively. FC and ZFC denote field-cooling and zero-field cooling curves, respectively.

Superconducting properties. The temperature dependence of resistivity around the temperature of liquid helium indicates further similarity between the superconducting Ti_4O_7 and γ-Ti_3O_5 films [Fig. 4(a) and (b), respectively]. The T_C of Ti_4O_7 and γ-Ti_3O_5 were 3.0 K and 7.1 K for $T_{C,onset}$, 2.7 K and 6.6 K for $T_{C,mid}$, and 5.8 K and 2.5 K for $T_{C,zero}$, respectively. Note that the T_C of both films exceeded that of other simple-oxide superconductors in bulk [TiO ($T_C = 2.3$ K), NbO ($T_C \sim 1.4$ K), and SnO ($T_C = 1.4$ K under 9.3 GPa)][13–16]. We also note that enhancement of $T_C = \sim 7$ K in TiO films has been reported in recent[17]. The superconducting states were gradually degraded under applied magnetic fields. Here, the magnetic fields were applied perpendicular to the film surface. T_C shifted toward a lower temperature under a higher magnetic field, and the superconducting phase finally disappeared for the Ti_4O_7 film at above 2 K. As for the γ-Ti_3O_5 films, superconductivity remained robust even under 9 T. In addition, from the temperature dependence of magnetization measurements, where magnetic field was applied parallel to the film surface, clear diamagnetic signals were observed [insets of Fig. 4(a) and (b)], respectively. The observation of diamagnetic signals in field-cooling curves indicates the Meissner effect of bulk superconductivity inTi_4O_7 and γ-Ti_3O_5 films, and roles out major influences arising from impurity, filament, and/or surface states.

Discussion

Chakraverty *et al.* proposed a theory to predict Superconductivity in Ti_4O_7 with the largest λ_{ep} value[18–20]. Therefore, experimental verifications for superconductivity in bulk Ti_4O_7 were attempted by applying high pressures. However, no superconducting transition was observed under a hydrostatic pressure of up to 5.0 GPa, although the high-temperature metallic phase was extended down to 3 K[9,10]. Our first observation of superconductivity in a Ti_4O_7 film demonstrates the importance of the epitaxial thin film. Titanium-based simple oxides with various chemical formulae and polymorphisms easily transform from one to another, and subtle tuning of oxygen stoichiometry causes modulation of carrier density. Epitaxial growth on LSAT substrates enables us to stabilize the Magnéli phase. In fact, the γ-Ti_3O_5 and Ti_4O_7 films can also be grown on different substrates under the same growth conditions ($T_g = 900$ °C and $P_{O2} = 1 \times 10^{-7}$ Torr) (see Fig. S9 in Supplementary Information). The lack of these advantages would be inevitable for hidden superconducting phases in bulk specimens. The MIT of the stoichiometric Ti_4O_7 bulk is premised on the bipolaronic interaction[9–11]. Sharp increase in resistivity and hysteresis at the MIT are strong evidence for the bipolaron formation[9–11]. The insulating Ti_4O_7 film exhibiting such characteristics can be regarded as a bipolaronic insulator at low temperatures. For a bipolaronic system, the bipolaron density is a key parameter in the electronic phase diagram[19]. Our growth of Ti_4O_7 films under Ar atmosphere aims at inducing extra Ti 3*d* electrons by introducing oxygen vacancies which dilute the bipolaron density, resulting in the suppression of the insulating states. In fact, the inverse R_H of the superconducting film suggests suppression of the bipolaron formation [Fig. 3(a)]. Ti_4O_7 films grown on $MgAl_2O_4$ (100) substrates also exhibited superconductivity (see Figs S11 and S12 in Supplementary Information). Thus, the observed superconductivity is intrinsic to the Ti_4O_7 phase. Furthermore, superconductors composed of Mg, Al, Ti, and O with T_C of more than 3 K are not yet known, indicating that any elements from the substrates cannot induce the superconductivity in our samples.

For bulk γ-Ti_3O_5, the MIT occurs with the structural phase transition at ~240 K[7]. There was no sign of such a structural phase transition at the temperature in the resistivity curve of the γ-Ti_3O_5 film [Fig. 3(b)], suggesting that the metallic γ-phase was stabilized in an epitaxial thin film. The first-principle calculations revealed a one-dimensional conducting pathway along the *c*-axis arising from the density of states at the Fermi level[7]. The low-dimensional electronic structure would lead to the pairing of electrons at ~100 K where MIT occurred in γ-Ti_3O_5. On the other hand, the small number of studies on γ-Ti_3O_5 makes it difficult to discuss the strength of the electron–phonon interaction, the formation of bipolarons, and the density of states at the Fermi level. Further investigation will be necessary to reveal the origin of superconductivity as well as several electronic phase transitions.

In summary, we study new superconductors produced from Ti_4O_7 and γ-Ti_3O_5 films whose T_C are 3.0 and 7.1 K, respectively. The latter is one of the highest known values among simple oxides. Our investigations on the electronic properties and the previous theoretical prediction suggest that epitaxial stabilization and oxygen non-stoichiometry play key roles in the realization of superconductivity in the titanates.

Methods

Thin-Film Preparation. A TiO_x ceramic tablet was prepared using a conventional solid-state reaction method. Ti (3 N) and TiO_2 (4 N) powders with a molar ratio of 1:3 were mixed and pressed into a pellet. This was sintered at 1000 °C for 12 *h* in vacuum. Prior to the film growth, LSAT and α-Al_2O_3 substrates were annealed in air to obtain a step-and-terrace surface. The annealing conditions were 1200 °C for 3 *h* for $(LaAlO_3)_{0.3}$–$(SrAl_{0.5}Ta_{0.5}O_3)_{0.7}$ (LSAT), and 1100 °C for 3 *h* for α-Al_2O_3. The films were grown using PLD in an ultra-high-vacuum chamber. KrF excimer laser pulses (5 Hz, 2.0 J/cm^2) were focused on the TiO_x ceramics tablets. The growth temperature was set at 900 °C. The chamber pressure was controlled with the continuous flow of oxygen or Ar gas (6 N purity for both). Ar atoms in the chamber tend to scatter with the lighter oxygen, especially when mean free path of the gaseous species exceeds the target-substrate distance[21,22]. Therefore, introduction of Ar (oxygen) gas during the growth corresponds to reduction (oxidation) of the films. In fact, we have also grown TiO and Ti_2O_3 films using PLD in Ar atmosphere (see Fig. S1 in Supplementary Information)[8]. After the growth, the gas flow was stopped immediately, and the samples were quenched to room temperature.

Characterization of the thin films. Thickness of all the films was ~120 nm, as measured by a stylus profiler. The crystal structures of the films were characterized using XRD with Cu Kα_1 radiation (Rigaku, SmartLab) and synchrotron radiation at BL15XU in SPring-8. The photon energy of the synchrotron radiation was set at 15 keV ($\lambda = 0.826$ Å). The temperature dependence of resistivity was measured using a standard four-probe method with a physical properties measurement system (Quantum Design, PPMS). The temperature dependence of the Hall measurements was also measured using PPMS in a standard six-terminal geometry. The temperature dependence of magnetization was measured using magnetic properties measurement system (Quantum Design, MPMS).

References

1. Marezio, M., Mcwhan, D.B., Dernier, P. D. & Remeika, J.P. Structural aspects of the metal-insulator transitions in Ti_4O_7. *J. Sol. State Chem.* **6**, 213 (1973).
2. Lakkis, S., Schlenker, C., Chakraverty, B.K., Buder, R. & Marezio, M. Metal-insulator transition in Ti_4O_7 single crystals: Crystal characterization, specific heat, and electron paramagnetic resonance. *Phys. Rev. B* **14**, 1429 (1976).
3. Åsbrink, S. & Magnéli, A. Crystal structure studies on Trititanium Pentoxide, Ti_3O_5. *Acta Cryst.* **12**, 575 (1959).
4. Hong, S. –H. & Åsbrink, S. The structure of γ-Ti_3O_5 at 297 K. *Acta. Cryst.* **B38**, 2570 (1982).
5. Onoda, M. Phase transitions of Ti_3O_5. *J. Sol. State Chem.* **136**, 67 (1998).
6. Ohkoshi, S. *et al*. Synthesis of a metal oxide with a room-temperature photoreversible phase transition. *Nature Chem.* **2**, 539 (2010).
7. Tanaka, K. *et al*. Structural phase transition between γ-Ti_3O_5 and δ-Ti_3O_5 by breaking of one-dimensionally conducting pathway. *Cryst. Growth Des.* **15**, 653 (2015).
8. Kurokawa, H., Yoshimatsu, K., Sakata, O. & Ohtomo, A. Effects of phase fraction on superconductivity of low-valence eutectic titanate films. *J. Appl. Phys.* **122**, 055302 (2017).
9. Tonogai, T., Takagi, H., Murayama, C. & Mori, N. Metal-insulator transitions in Ti_4O_7: Pressure-induced melting of the electron pairs. *Rev. High Pressure Sci. Technol.* **7**, 453 (1998).
10. Ueda, H., Kitazawa, K., Takagi, H. & Matsumoto, T. Strong carrier concentration dependence of pressure effects on bipolaronic transitions in Magnéli phase Ti_nO_{2n-1} ($n = 4, 5, 6$). *J. Phys. Soc. Jpn.* **71**, 1506 (2002).
11. Mareizo, M., Mcwhan, D. B., Dernier, P. D. & Remeika, J. P. Charge localization at metal-insulator transitions in Ti_4O_7 and V_4O_7. *Phys. Rev. Lett.* **28**, 1390 (1972).
12. Schlenker, C., Ahmed, S., Buder, R. & Gourmala, M. Metal-insulator transitions and phase diagram of $(T_{i1-x}V_x)_4O_7$: electrical, calorimetric, magnetic and EPRstudies. . *J. Phys. C: Solid State Phys.* **12**, 3503 (1979).
13. Doyle, N. J., Hulm, J. K., Jones, C. K., Miller, R. C. & Taylor, A. Vacancies and superconductivity in titanium monoxide. *Phys. Lett.* **26A**, 604 (1968).
14. Morin, F. J. Oxides which show a metal-to-insulator transition at the Neel temperature. *Phys. Rev. Lett.* **3**, 34 (1959).
15. Hulm, J. K., Jones, C. K., Hein, R. A. & Gibson, J. W. Superconductivity in the TiO and NbO system. *J. Low Temp. Phys.* **7**, 291 (1972).
16. Forthaus, M. K. *et al*. Superconductivity in SnO: a nonmagnetic analog to Fe-based superconductors? *Phys. Rev. Lett.* **105**, 157001 (2010).
17. Zhang, C. *et al*. Enhanced superconductivity in TiO epitaxial thin films. *npj Quantum Materials* **2**, 2 (2017).
18. Chakraverty, B. K. Possibility of insulator to superconductor phase transition. *J. de Physique Lettres* **40**, 99 (1979).
19. Jongh, L. J. D. A comparative study of (bi)polaronic (super)conductivity in high- and low- T_C superconducting oxides. *Physica C* **152**, 171 (1988).
20. Micnas, R., Ranninger, J. & Robaszkiewicz, S. Superconductivity in narrow-band systems with local nonretarded attractive interactions. *Rev. Mod. Phys.* **62**, 113 (1990).
21. Schou, J. Physical aspects of the pulsed laser deposition technique: the stoichiometric transfer of material from target to film. *Appl. Surf. Sci.* **255**, 5191 (2009).
22. Ojeda-G-P, A., Schneider, C. W., Döbeli, M., Lippert, T. & Wokaun, A. The importance of pressure and mass ratios when depositing multi-element oxide thin films by pulsed laser deposition. *Appl. Surf. Sci.* **389**, 126 (2016).

Acknowledgements

The authors greatly thank Prof. S. Saito, Dr. S. Okamoto, Dr. T. Koretsune, and Dr. R. Arita for their useful discussion. The authors also thank M. Azuma and H. Hojo for assistance of magnetization measurements. The Synchrotron XRD measurements were performed under the approval of the NIMS Synchrotron x-ray station at SPring-8 (Proposal No. 2015B4700). The authors are also grateful to K. Yokoyama, S. Takeda, K. Kagoshima, and J. Matsui, University of Hyogo, for their technical contribution and to Y. Shimada and Y. Katsuya for their technical support. This work was partly supported by MEXT Elements Strategy Initiative to Form Core Research Centre and a Grant-in-Aid for Scientific Research (Nos. 15H03881 and 16H05983) from the Japan Society for the Promotion of Science Foundation.

Author Contributions

K.Y. performed the experiments and analysed experimental data. O.S. supervised the synchrotron X-ray diffraction measurements. All authors discussed the results and wrote the manuscript. A.O. supervised the project.

Additional Information

Supplementary information accompanies this paper at https://doi.org/10.1038/s41598-017-12815-4.

Competing Interests: The authors declare that they have no competing interests.

Publisher's note: Springer Nature remains neutral with regard to jurisdictional claims in published maps and institutional affiliations.